Biochimica et Biophysica Acta 1850 (2015) 373–384

Contents lists available at ScienceDirect

Biochimica et Biophysica Acta

journal homepage: www.elsevier.com/locate/bbagen

Basal Flt1 tyrosine kinase activity is a positive regulator of endothelial survival and vascularization during zebrafish embryogenesis

Shang Li [a], Xue Lin Zhou [b], Yuan Ye Dang [a], Yiu Wa Kwan [b], Shun Wan Chan [c], George Pak Heng Leung [c], Simon Ming-Yuen Lee [a,*], Maggie Pui Man Hoi [a,*]

[a] State Key Laboratory of Quality Research in Chinese Medicine and Institute of Chinese Medical Sciences, University of Macau, Avenida da Universidade, Taipa, Macao, China
[b] School of Biomedical Sciences, Faculty of Medicine, The Chinese University of Hong Kong, Shatin, N.T., Hong Kong, China
[c] State Key Laboratory of Chinese Medicine and Molecular Pharmacology, Department of Applied Biology and Chemical Technology, The Hong Kong Polytechnic University, Hong Kong, China
[d] Department of Pharmacology and Pharmacy, Faculty of Medicine, The University of Hong Kong, Hong Kong, China

ARTICLE INFO

Article history:
Received 30 April 2014
Received in revised form 23 September 2014
Accepted 22 October 2014
Available online 29 October 2014

Keywords:
Flt1
VEGF receptor inhibitor
Calycosin
Zebrafish
Endothelial cell
Molecular docking

ABSTRACT

Background: The role of Kdr (VEGFR-2/Flk-1) in vascular formation has been well described, but the role of Flt1 (VEGFR-1) is not well studied and is generally considered as a decoy receptor for trapping VEGF.
Methods: The effects of VEGFR1/2 kinase inhibitor (VRI) and calycosin on Flt1 tyrosine kinase (TK) activity were evaluated by molecular docking, enzymatic inhibition assay, protein co-immunoprecipitation and siRNA gene knock-down analysis in HUVECs. Toxicities of the chemicals were examined using HUVECs viability. Their effects on angiogenesis and vessel formation were furthered studied in HUVECs *in vitro* and *Tg(fli-1:EGFP)* zebrafish *in vivo*. The gene and protein expression of VEGF and VEGF receptors were investigated by quantitative RT-PCR and Western blot.
Results: VRI strongly inhibited physiological functions of both VEGF receptors and suppressed endothelial cell survival. This resulted in blood vessel loss in zebrafish embryos. Interestingly, calycosin co-treatment impeded VRI-induced blood vessel loss. Docking and kinase inhibition assay revealed that calycosin competed with VRI for the tyrosine kinase domain of Flt1 without affecting ATP binding. On the contrary, calycosin did not affect the interaction between VRI and Kdr-TK. Consistent with these results, calycosin counteracted the inhibition of Flt1-TK and PI3K phosphorylation induced by VRI in HUVECs. Further studies in vitro and in vivo showed that the minimizing effect of calycosin on VRI-mediated endothelial cytotoxicity was blocked by wortmannin (a PI3K inhibitor). The impeding effect of calycosin on VRI-induced blood vessel loss was absent in zebrafish embryos injected with Flt1 MO.
Conclusions: Flt1-tyrosine kinase (TK) activity contributed significantly in endothelial cells survival and vascular development during embryo angiogenesis in zebrafish by engaging PI3K/Akt pathway.
General significance: The roles of Flt1 activity in endothelial cell survival in physiological vascular formation may have been previously under-appreciated.

1. Introduction

The pivotal roles of vascular endothelial growth factors (VEGFs) and the two VEGF receptors Flt1 (also known as VEGFR-1) and Kdr (also known as VEGFR-2/Flk-1) in the regulation of blood vessel formation during vertebrate development have been well described [1–4]. Flt1 has a higher affinity for VEGF-A than Kdr [5,6], but its tyrosine kinase activity is weakly induced resulting in only modest mitogenic signal for endothelial cell [3,7]. In mice, gene targeting studies showed that *Flt1*$^{-/-}$ mouse embryos did not survive through mid-gestation with increased endothelial cell proliferation and disorganized vascular system possibly due to up-regulation of Kdr signaling [2,3], but the deletion of the intracellular tyrosine kinase (TK) domain of Flt1 did not reduce vascular development at the early stage of embryogenesis [8]. Thus, Flt1 has generally been considered as a negative regulator in developmental angiogenesis to regulate Kdr signaling [9].

Similar VEGF signaling pathways have also been observed for vascular development in zebrafish embryos. Morpholinos targeting Kdr in zebrafish resulted in vascular defects particularly in intersegmental vessels (ISV) [10]. Interestingly, zebrafish Kdr morphants display much less severe vascular defects than *Kdr*$^{-/-}$ mice [10]. Besides, it has been observed that the suppression of both Kdr and Flt1 activities with non-specific VEGFR inhibitor PTK787/ZK222584 caused pronounced defects in vascular formation and vessel function [11]. Flt1-mediated PI3K (phosphoinositide 3-kinase)/Akt signaling pathway has been implicated to be involved in endothelial cell differentiation, migration and vascular tube organization [12–14]. It is thus possible that Flt1 tyrosine kinase activity might have a more significant role in zebrafish embryo vascular development. Five tyrosine autophosphorylation sites

* Corresponding authors. Tel.: +853 88224876; fax: +853 28841358.
E-mail addresses: simonlee@umac.mo (S.M.-Y. Lee), maghoi@umac.mo (M.P.M. Hoi).

http://dx.doi.org/10.1016/j.bbagen.2014.10.023
0304-4165/

(Tyr-1169, Tyr-1213, Tyr-1242, Tyr-1327 and Tyr-1333) have been identified in the intracellular domain of Flt1 [15]. Tyr-1213 has been shown to bind to a variety of Src homology 2 (SH2) domain-containing proteins including the p85 subunit of PI3K (phosphoinositide 3-kinase), PLC-γ (phospholipase C-γ), GRB-2 (growth factor receptor-bound protein 2), Nck (non-catalytic region of tyrosine kinase adaptor protein) and SHP-2 (SH2-domain-containing protein tyrosine phosphatase 2) [15–17].

In the present study, we focused on the role of Flt1 in zebrafish embryonic angiogenesis and endothelial cell function. We observed that blockade of both Flt1 and Kdr kinase activities by VRI (VEGF Receptor Kinase Inhibitor II) completely abolished the formation of the segmental vessels in the trunk of zebrafish embryos, whereas selective Kdr inhibitors produced a less severe reduction of angiogenesis. By employing molecular docking and enzymatic assays, we discovered that calycosin, an isoflavone with proangiogenic properties [18,19], could counteract the VRI-induced inhibition on Flt1 autophosphorylation and the downstream PI3K/Akt pathway. In addition, calycosin co-treatment reduced VRI-induced blood vessel defects in zebrafish embryos, which was absent in zebrafish embryos injected with Flt1 morpholino (MO). These results suggested that basal Flt1/PI3K/Akt activity is a positive regulator for endothelial cell survival, development and blood vessel formation in zebrafish embryos, potentially playing an essential role in developmental angiogenesis.

2. Material and method

2.1. Ethics statement

All animal experiments were conducted according to the ethical guidelines of Institute of Chinese Medical Sciences (ICMS), University of Macau and the protocol was approved by Institute of Chinese Medical Sciences — Animal Ethics Committee (ICMS—AEC) of the University of Macau (Permit Number: 20120601).

2.2. Chemicals and reagents

Kaighn's modification of Ham's F12 medium (F-12K), fetal bovine serum (FBS), phosphate-buffered saline (PBS), penicillin–streptomycin (PS) and 0.25% (w/v) trypsin/1 mM EDTA were all purchased from Invitrogen (Carlsbad, CA, USA). Endothelial cell growth supplement (ECGS), heparin, and gelatin were supplied by Sigma (St Louis, MO). ERK activation inhibitor peptide II was obtained from Biocalchem (Darmstadt, Germany). Recombinant Human $VEGF_{165}$ (VEGF) was obtained from R&D Systems (Minneapolis, MN). Anti-p-PI3K antibody, anti-PI3K antibody and goat anti-rabbit IgG HRP-conjugated antibody were all purchased from Cell Signaling Technology (Beverly, MA). Anti-phospho-Flt-1 (Tyr1213) antibody was purchased from Millipore. Anti-Flt-1 was purchased from Santa Cruz and Biocompare. Acetonitrile and methanol were of HPLC grade from Merck (Darmstadt, Germany), and formic acid was of HPLC grade (Tedia, USA); deionized water (18.2 MΩ) was purified using a Milli-Q system (Millipore, Bedford, MA, USA). Dimethyl sulfoxide (DMSO) was acquired from SIGMA and the calycosin (≥98%) was purchased from Forever-biotech Company, Shanghai, Cas No. 20575-57-9. Calycosin was dissolved in DMSO to form a 100 mM solution. VEGFR tyrosine kinase inhibitor II (VRI) was purchased from Calbiochem Company and was dissolved in DMSO to form a 100 μM solution.

2.3. Zebrafish embryo preparation and drug treatment

Zebrafish embryo preparation was done as described in our previous paper [20]. Transgenic *Tg*(*fli-1*:*EGFP*) zebrafish were kept separately with a 14 h light/10 h dark cycle under standard conditions [20]. Zebrafish embryos were generated by natural pair-wise mating (3–12 months old) and were raised at 28.5 °C in embryo water. 24 hpf zebrafish embryos were collected, distributed into a 12-well microplate with 15 fish in each well and co-treated with 300 nM VRI (VEGFR tyrosine kinase inhibitor II) and 12.5, 25, 50, 100, 200 μM calycosin for 24 and 48 h. Embryos receiving embryo water with 0.1% DMSO served as a vehicle control and were equivalent to no treatment. All of these experiments were repeated three times, with 15 embryos per group.

2.4. Morphological observation of zebrafish

Zebrafish embryos were removed from microplates after drug treatment and observed for viability and gross morphological changes under a fluorescence microscope (Olympus IX81 Motorized Inverted Microscope, Japan) equipped with a digital camera (DP controller, Soft Imaging System, Olympus). The sprouting vessels in intersegmental vessel (ISV) indicate ISV generated from the dorsal aorta (DA) but disconnected with dorsal longitudinal anastomotic vessel (DLAV). The intact vessels in ISVs indicate that ISV is generated from the DA and connected with DLAV. The number of sprouting vessels and intact vessels in ISV was counted in each inhibitor treatment group. SV (sprouting vessels of ISV) IC50: half maximal sprouting ISV inhibitory concentration of inhibitors; IV (intact vessels of ISV): half maximal intact vessels of ISV inhibitory concentration of inhibitors; images were analyzed with Axiovision 4.2, Adobe Photoshop 7.0 and Image J.

2.5. Detection of apoptosis in zebrafish embryos

24 hpf *Tg*(*fli-1*:*EGFP*) was treated with 300 nM VRI and/or 100 μM calycosin for 8 h. Embryos were fixed in 4% paraformaldehyde overnight at 4 °C and stored in 100% ethanol at −20 °C until further processing. For apoptosis studies, embryos were first rehydrated with decreasing concentrations of ethanol, washed with PBST (PBS, 0.1% Tween 20), treated with proteinase K (10 mg/ml) at 37 °C for 30 to 60 min, refixed with 4% paraformaldehyde, and washed in PBST. TUNEL staining was performed with the ApopTag® Red In Situ Apoptosis Detection Kit (Chemicon). Embryos were visualized by fluorescence microscope (Olympus IX81 Motorized Inverted Microscope, Japan), and pictures were taken under green fluorescence Tg(Fli:eGFP) and red fluorescence (apoptotic cells) with a digital camera (DP controller, Soft Imaging System, Olympus).

2.6. Total RNA extraction, reverse transcription, and real-time PCR

Zebrafish embryos (wild type) at 24 hpf were treated with 30, 100, and 300 nM VRI (VEGFR tyrosine kinase inhibitor II) and/or 100 μM calycosin or embryo medium (with 0.1% DMSO as blank control) for 24 h. Total RNA was extracted from 30 zebrafish embryos of each treatment group using the RNeasy Mini Kit (Qiagen, USA) in accordance with the manufacturer's instructions. RNA was reverse transcribed to single-strand cDNA using SuperScript™ III First-Strand Synthesis System for RT-PCR (Invitrogen™, USA), followed by real-time PCR using the TaqMan® Universal PCR Master Mix and 250 nM TaqMan primers for zebrafish *bactin1*, *flt1*, *Kdr*, *Kdrl*, *vwf*, *cdh5* and *vegfa* (Applied Biosystems, USA) in the ABI 7500 Real-Time PCR System (Applied Biosystems). The expression of *flt1*, *Kdr*, *Kdrl*, *vwf*, *cdh5* and *vegfa* mRNA was normalized to the amount of *bactin1*, using the relative quantification method described by the manufacturer.

The zebrafish *bactin1* primers were 5′-CAAGATTCCATACCCAGG AAGGA-3′ (F) and 5′-CAAGATTCCATACCCAGGAAGGA-3′(R) (Applied Biosystems, USA).

The zebrafish *Kdrl* primers were 5′-GACCATAAAACAAGTGAG GCAGAAG-3′ (F) and 5′-CTCCTGGTTTGACAGAGCGATA-3′(R) (Applied Biosystems, USA).

The zebrafish *Kdr* primers were 5′-CAAGTAACTCGTTTTCTCAACC TAAGC-3′ (F) and 5′-GGTCTGCTACACAACGCATTATAAC-3′(R) (Applied Biosystems, USA).

The zebrafish *cdh5* primers were 5′-CCAAACAGAGTACACGTTTA GCGT-3′ (F) and 5′-ACTATCTGGGTCTTTTGCTGAAACA-3′(R) (Applied Biosystems, USA).

The zebrafish *flt1* primers were 5′-AACTCACAGACCAGTGAACA AGATC-3′ (F) and 5′-GCCCTGTAACGTGTGCACTAAA-3′(R) (Applied Biosystems, USA).

The zebrafish *von Willebrand factor* (*vwf*) primers were 5′-CTCCGTTT GACCGCAAAA-3′ (F) and 5′-ACAGCAGGTGTCTCCGATCT-3′ (R) (Roche, USA).

The zebrafish VEGFA2 (*vegfa*) primers were 5′-GATGTGATTCCCTT CATGGATGTGT-3′ (F) and 5′-GGATACTCCTGGATGATGTCTACCA-3′ (R) (Applied Biosystems, USA).

2.7. Apparatus and chromatographic conditions

Chromatographic analysis was performed on an Agilent 1200 series LC system (Agilent, Germany) equipped with a quaternary pump and a thermostatically controlled column apartment. Chromatographic separation was carried out at 25 °C on a ZORBAX C-18 column (250 mm × 4.6 mm, 5 μm) and a ZORBAXC-18 guard column (12.5 mm × 4.6 mm, 5 μm). The mobile phase consisted of 1% formic acid water (A) and acetonitrile (B) using a gradient elution. The gradient condition is: 0–33 min, 5–39% B; 33–40 min, 39–100% B; the flow rate was 1 ml/min and the injection volume was 10 μl. The detection wavelength was set at 254 nm.

2.8. Molecular docking study

Molecular docking analysis was performed to investigate the binding modes of ATP, VRI and calycosin to human VEGF receptor 1 (PDB code 3HNG) and VEGF receptor 2 (PDB code 2OH4) which were obtained from the Protein Data Bank. The software AutoDock Vina v.1.0.2 was used for all dockings with the default values [21]. The size of the grid box was set as 20 Å × 20 Å × 20 Å, encompassing the ATP binding site of human VEGFR 1 and VEGFR 2 [22]. The binding modes with lowest binding free energy were chosen as the optimum docking conformation. The binding results were simulated by PyMOL Molecular

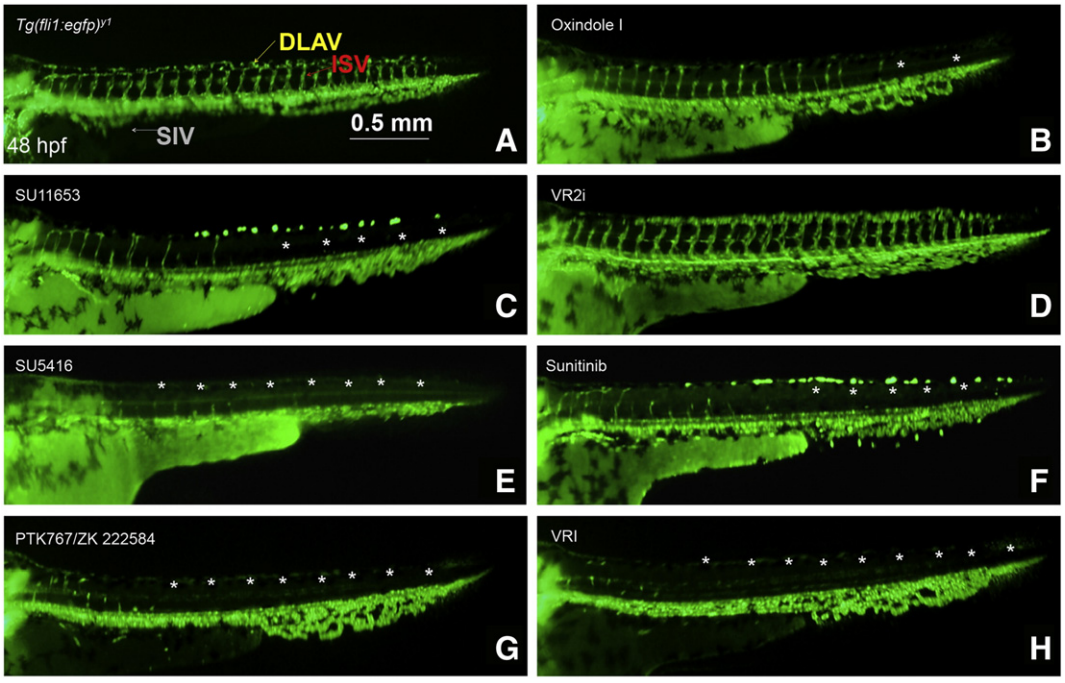

I

VEGFR inhibitors	Inhibitor specificity	Concentration of inhibitors (μM)						SV IC50	IV IC50
		0.1	0.3	1	3	10	30	μM	μM
Oxindole I	Kdr	-	-	*	**	Toxic		2.752±0.32	2.3±0.27
SU11652	Kdr	-	*	**	**	Toxic		1.03±0.2	0.711±0.13
VR2i	Kdr	-	-	-	*	**	Toxic	8.584±0.52	5.709±0.36
SU5416	Flt1/Kdr	-	-	*	**	**	Toxic	2.706±0.19	1.413±0.15
Sunitinib	Flt1/Kdr	-	*	**	***	Toxic		0.731±0.08	0.373±0.04
PTK787/ZK 222584	Flt1/Kdr	*	**	***	***	***	Toxic	0.265±0.02	0.167±0.01
VRI	Flt1/Kdr	**	***	***	***	***	Toxic	0.185±0.01	0.091±0.01

Fig. 1. The anti-angiogenesis effects of VEGF receptor inhibitors. Zebrafish embryos (24 hpf) were treated for 24 h with (A) 0.1% DMSO (control), (B) 1 μM Oxindole I, (C) 1 μM SU11652, (D) 1 μM VR2i, (E) 1 μM SU5416, (F) 1 μM Sunitinib, (G) 1 μM PTK767/ZK 222584 and (H) 1 μM VRI. White asterisks indicated loss of vessels in intersegmental vessel (ISV) and dorsal longitudinal anastomotic vessel (DLAV) region. (I) Semi-quantitative results of anti-angiogenic effects of various inhibitors. SV (sprouting vessels of ISVs) IC50: half maximal sprouting ISV inhibitory concentration of inhibitors; IV (intact vessels of ISVs): half maximal intact vessels of ISV inhibitory concentration of inhibitors; —, inactive; *, <50%; **, 50 — 90%; ***, >90% inhibition as compared with control.

Graphics System Version 1.3 (Schrödinger, OR, USA) and Discovery Studio Visualizer (Accelrys, Inc., CA, USA), respectively.

2.9. VEGF receptor kinase inhibition assay

Flt1 and Kdr tyrosine kinase inhibition assay was performed using the Phosphotyrosine HTRF® Assay kit (Cat No. 17-10015) and active Flt1 (Millipore, Cat No. 14-562) and KDR (Millipore, Cat No. 14-630) peptide. In brief, all of the reactions were performed in a 96-well black assay plate at 37 °C, and the incubation time was set to 60 min for VRI and calycosin. In this case, detection reagent incubates for 60 min at room temperature. At the end of incubation, TR-FRET ratio of fluorescence at 660–50 nm and 620–35 nm (excitation at 330 nm) was measured on a fluorescence plate reader (Roche).

2.10. Transfection of short interfering RNA (siRNA)

Transfection was performed with a culture cellular density reaching 50–70% confluence with SignalSilence® Akt siRNA I, II or SignalSilence® Control siRNA (CST, Beverly, MA) according to the manufacturer's instructions. Briefly, Opti-MEM® Reduced Serum Medium (Life Technologies, Cat No. 31985062) was mixed with Akt siRNA or Control siRNA (CST) for 5 min incubation in room temperature. Then the mixture and Lipofectamine® LTX with Plus™ Reagent (Life Technologies, Cat No. 15338100) were mixed and incubated for 20 min at room temperature and diluted with complete culture medium. The culture medium of the cells was aspirated and replaced with the diluted transfection complex mixture. The cells transfected were used in the indicated assays.

2.11. Western blotting analysis

Cells were treated with 0.1, 0.3, 1 μM VRI and/or 100 μM calycosin for 1 h, then stimulated with 40 ng/ml VEGF for 15 min. Cells receiving DMSO (0.1%) served as vehicle control and were equivalent to no treatment. Cells were then washed with PBS and lysed for 30 min on ice with lysis buffer (0.5 M NaCl, 50 mM Tris, 1 mM EDTA, 0.05% SDS, 0.5% Triton X-100, 1 mM PMSF, pH 7.4). Cell lysates were centrifuged at 12500 ×*g* for 20 min at 4 °C. Protein concentrations in the supernatants were measured using the bicinchoninic acid assay (Pierce, Rockford, IL). Supernatants were electrophoresed on 8% SDS-PAGE, and transferred to polyvinylidene difluoride (PVDF) membranes, which were then blocked with 5% non-fat milk. Immunoblot analysis was undertaken by incubation with anti-p-Flt1 Tyr1213, anti-Flt1, anti-p-PI3K, anti-PI3K and anti-β-actin antibody at 4 °C overnight. After washing,

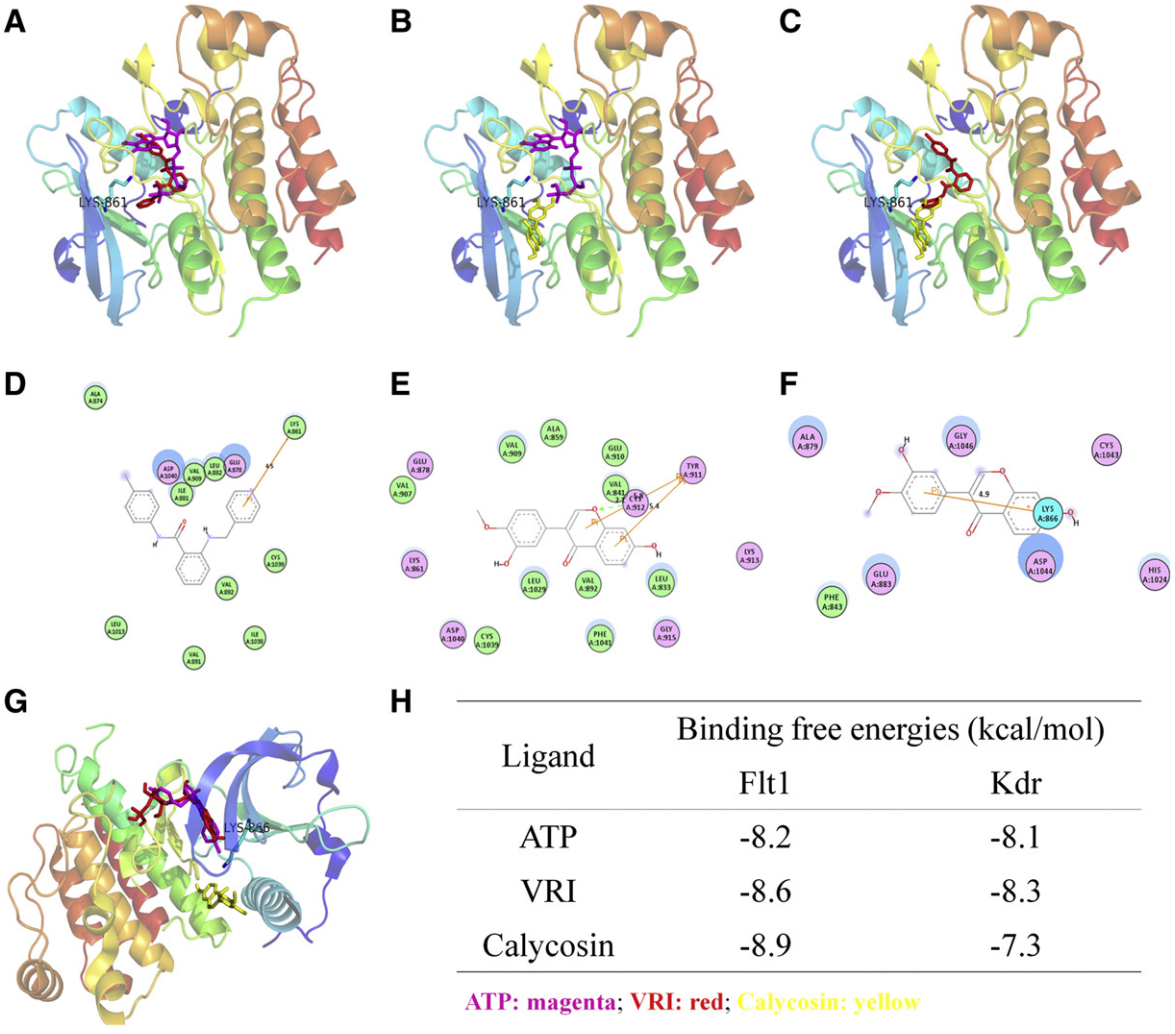

Ligand	Binding free energies (kcal/mol)	
	Flt1	Kdr
ATP	-8.2	-8.1
VRI	-8.6	-8.3
Calycosin	-8.9	-7.3

ATP: magenta; VRI: red; Calycosin: yellow

Fig. 2. Three-dimensional structural models of compounds (A) ATP and VRI, (B) ATP and calycosin, and (C) VRI and calycosin, into Flt1 kinase derived from the docking simulations. Interactions from molecular docking between (D) Flt1 ATP-binding site and VRI, (E) Flt1 ATP-binding site and calycosin, (F) Kdr ATP-binding site and VRI, and (G) Kdr ATP-binding site and calycosin. Van der Waals (green); polar (magenta); and pi–pi interaction (yellow). Green and blue arrows represent H-bonding with amino acid main chain and side chain respectively. (H) Logarithm of free binding energies (kcal/mol) of ligands to the ATP-binding site of Flt1 (PDB code 3HNG) and Kdr (PDB code 2OH4).

membranes were incubated for 1 h at room temperature with horseradish peroxidase-conjugated goat anti-rabbit IgG. Proteins were detected using an advanced enhanced ECL system (GE Healthcare, Little Chalfont, Buckinghamshire, UK). Semi-quantifications were performed with densitometric analysis by Quantity One software.

2.12. Protein extraction with deyolk for Western blot

Cholate extraction buffer was prepared with 10 mM Tris pH ~ 8.0, 2% Sodium Deoxycholate, and protease inhibitor cocktail. Treated embryos were washed with ice-cold 1 × PBS. Manually deyolk using a P200 pipet tip by pipetting three to five times in ice-cold 1 × PBS. Then the deyolked embryos were washed with ice-cold 1 × PBS and spin down embryos and discard suspensions in small microcentrifuges. Zebrafish embryos were homogenized in cholate extraction buffer on ice. Samples were stored at −80 °C and thaw for Western blot analysis.

2.13. Morpholino injections

Morpholino antisense oligonucleotides were purchased from Gene-Tools, LLC (Philomath, OR). A 1 nl volume of 2 mM morpholino or control morpholino (Gene-Tools, Philomath, OR) was injected into the yolk of transgenic *Tg* (*fli-1*:*EGFP*)^{y1} embryos (approximately 3 ng Flt1 MO) at the one-cell stage. The sequence of the injected translation-blocking target morpholino was referred with the previous study [23]: flt1: ATG blocking MO, 5`-ATATCGAACATTCTCTTGGTCTTGC-3` (Flt1MO, 3 ng); standard control MO, 5`-CTCTTACCTCAGTTACAATTTA TA-3` (control MO, 3 ng). All injected embryos were photographed live under a fluorescence microscope (Olympus IX81 Motorized Inverted Microscope, Japan) using an Olympus DP controller, and the Soft Imaging System software package.

2.14. Protein co-immunoprecipitation

Cells were grown in 6-well plates as above, lysed with lysis buffer (0.5 M NaCl, 50 mM Tris, 1 mM EDTA, 0.05% SDS, 0.5% Triton X-100, 1 mM PMSF, pH 7.4). Cell lysates were centrifuged at 12500 ×*g* for 20 min at 4 °C. 20 μg lysate protein was saved as total protein control. The rest of the lysate protein (30 μg) from each well was immunoprecipitated with Protein G Dynabeads (Invitrogen) charged with anti-p-Try antibody (sc-7020, Santa Cruz Biotechnology). Precipitates were washed with lysis buffer and eluted with Laemmli sample buffer and handled as above for Western blotting for Flt1 and PI3K.

2.15. Statistical analysis

Each experiment was done in triplicate. The mean and standard deviations were compared using Student's t-test with the following statistical criteria: $p < 0.05$, significant; $p < 0.01$, highly significant; $P < 0.001$ extremely significant. All relevant data are presented as mean ± SD.

3. Results

3.1. Blockade of both Flt1 and Kdr activities caused more severe reduction in angiogenesis than selective blockade of Kdr in zebrafish embryos

The anti-angiogenic effects of various VEGF receptor inhibitors [24–29] were evaluated in 48 hpf (hour post-fertilization) transgenic *Tg*(*fli1*:*EGFP*)^{y1} zebrafish embryos. Fig. 1(A to H) showed that the formation of intersegmental vessels (ISVs) was inhibited to different degrees after the treatments of various VEGF receptor inhibitors for 24 h. Fig. 1(I) represented semi-quantitative results of the anti-angiogenic effects of various inhibitors. It was observed that non-specific inhibitors, which block the activities of both Flt1 and Kdr, were more potent in mediating blood vessel loss in zebrafish embryo (VRI > PTK767/ZK222584 > Sunitinib > SU5416) than Kdr specific inhibitors (SU11652 > Oxindole I > VR2i). Among the inhibitors VRI displayed the best potency in mediating the anti-angiogenic effects (inhibition of sprouting vessel formation and intersegmental vessel formation), and was thus chosen for further study.

3.2. Identification of calycosin as a ligand at Flt1 by molecular docking analysis and enzymatic assay

Previous studies showed that calycosin possesses proangiogenic properties via VEGF signaling pathway [18]. Therefore, we further studied its interaction at Flt1 and Kdr with molecular docking analysis. We revealed that calycosin behaved as a competitive ligand at Flt1 against VRI without interfering the binding of ATP. VRI interfered with ATP-binding at Flt1 via pi–pi interaction with Lys 861 at a distance of 4.5 Å and to a lesser extent with polar and van der Waals interactions (Figs. 2A and D). VRI displayed similar binding conformation as ATP at Flt1 and exhibited higher binding free energy (−8.6 kcal/mol) than ATP (−8.2 kcal/mol), thus VRI behaves as a competitive inhibitor of ATP at Flt1. More interestingly, calycosin-binding site at Flt1 was predicted to partly overlap with the VRI-binding site without interfering ATP-binding (Figs. 2B and C). Moreover, calycosin exhibited the highest binding free energy at Flt1 (−8.9 kcal/mol), mainly via pi–pi interaction with Tyr 911 and to a lesser extent via polar and van der Waals interactions (Fig. 2E). This data suggests that calycosin is a competitor of VRI and could stop VRI from binding Flt1 without affecting Flt1-TK (tyrosine kinase) activity. On the other hand, at Kdr VRI was predicted to compete at the ATP-binding site with higher affinity (−8.3 kcal/mol) than ATP (−8.1 kcal/mol), providing further evidence for VRI as an inhibitor of Kdr-TK activity [30,31]. Calycosin exhibited low affinity (−7.3 kcal/mol) at a site in the activation segment of Kdr away from ATP–VRI interaction via sigma–pi interaction with Lys 866 in a distance of 4.9 Å (Figs. 2F and G).

The underlying mechanisms of VRI and calycosin at Flt1 and Kdr were further evaluated by in vitro enzymatic assays (Fig. 3). VRI

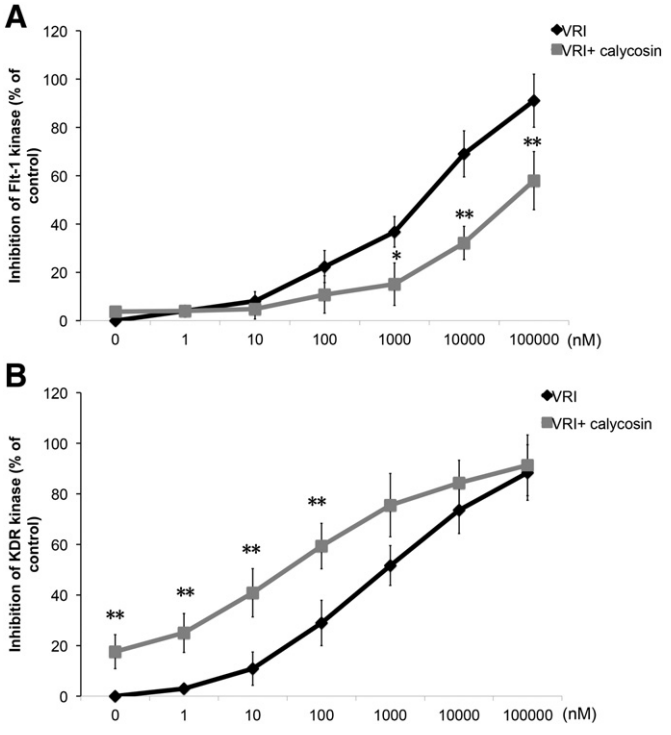

Fig. 3. Calycosin (100 μM) co-treatment attenuated VRI-induced inhibition of Flt1 tyrosine kinase activity but not Kdr. In vitro enzymatic assays of ATP-stimulated Flt1-tyrosine kinase (TK) and Kdr-TK activation. VRI induced inhibition in both Flt1-Tk (A) and Kdr-TK (B). $^{*}P < 0.05$, $^{**}P < 0.01$, $^{***}P < 0.001$ vs VRI only treatment.

significantly inhibited ATP-stimulated tyrosine kinase (TK) activities of both Flt1 and Kdr. In agreement with molecular docking data, the co-treatment of calycosin significantly attenuated the VRI-induced Flk1-TK inhibition (Fig. 3). This effect was not observed for Kdr. It also was observed that the inhibition of VRI at Kdr was enhanced by the co-treatment of calycosin. One possible explanation is that calycosin binding to Kdr did not affect its kinase activity but might induce conformational changes at the receptor at a site different from VRI, thus influencing the effect of VRI. Based on this analysis; we employed calycosin as competitive ligand to abolish the VRI-induced inhibition on ATP-dependent Flt1-TK activation.

3.3. Flt1-PI3K autophosphorylation enables endothelial cell survival in HUVECs

VEGF did not induce Flt1 tyrosine phosphorylation (Suppl. Fig. 1) whereas five tyrosine residues (1169, 1213, 1242, 1327 and 1333) of Flt1 were reported previously as autophosphorylation sites [15]. In the present study, we observed that quiescent HUVECs (human umbilical endothelial cells) treated with VRI (1 h) resulted in the inhibition of tyrosine kinase activity (Fig. 4A), autophosphorylation 1213 site of Flt1 tyrosine residues and PI3 kinase activity (Fig. 4B–C). The co-treatment of calycosin abrogated the inhibitory effects of VRI on Flt1 and PI3K phosphorylation. In contrast, VEGF significantly stimulated Kdr tyrosine phosphorylation, which was potently inhibited by VRI but not affected by calycosin co-treatment (Fig. 4E). VEGF receptors and PI3K signaling pathways have been well described in the involvement of endothelial cell survival. In line with this, Fig. 5 showed that VRI treatment (24 h) dose-dependently induced cytotoxicity and cell death in HUVECs as evaluated by XTT and LDH assays. More interestingly, we observed that calycosin co-treatment with VRI was able to stop the release of lactate dehydrogenase (LDH) and prevented cell death in HUVEC induced by VRI (Fig. 5A and C). In contrast, treatment with VEGF was unable to affect VRI-mediated cytotoxicity in HUVECs (Fig. 5B and D). Furthermore, as shown in Fig. 6, these effects of calycosin were significantly inhibited by wortmannin (a specific PI3K inhibitor; Stein et al., 2000) (100 nM) or AKT siRNA. These results suggested that calycosin mediated its effect mainly by competing

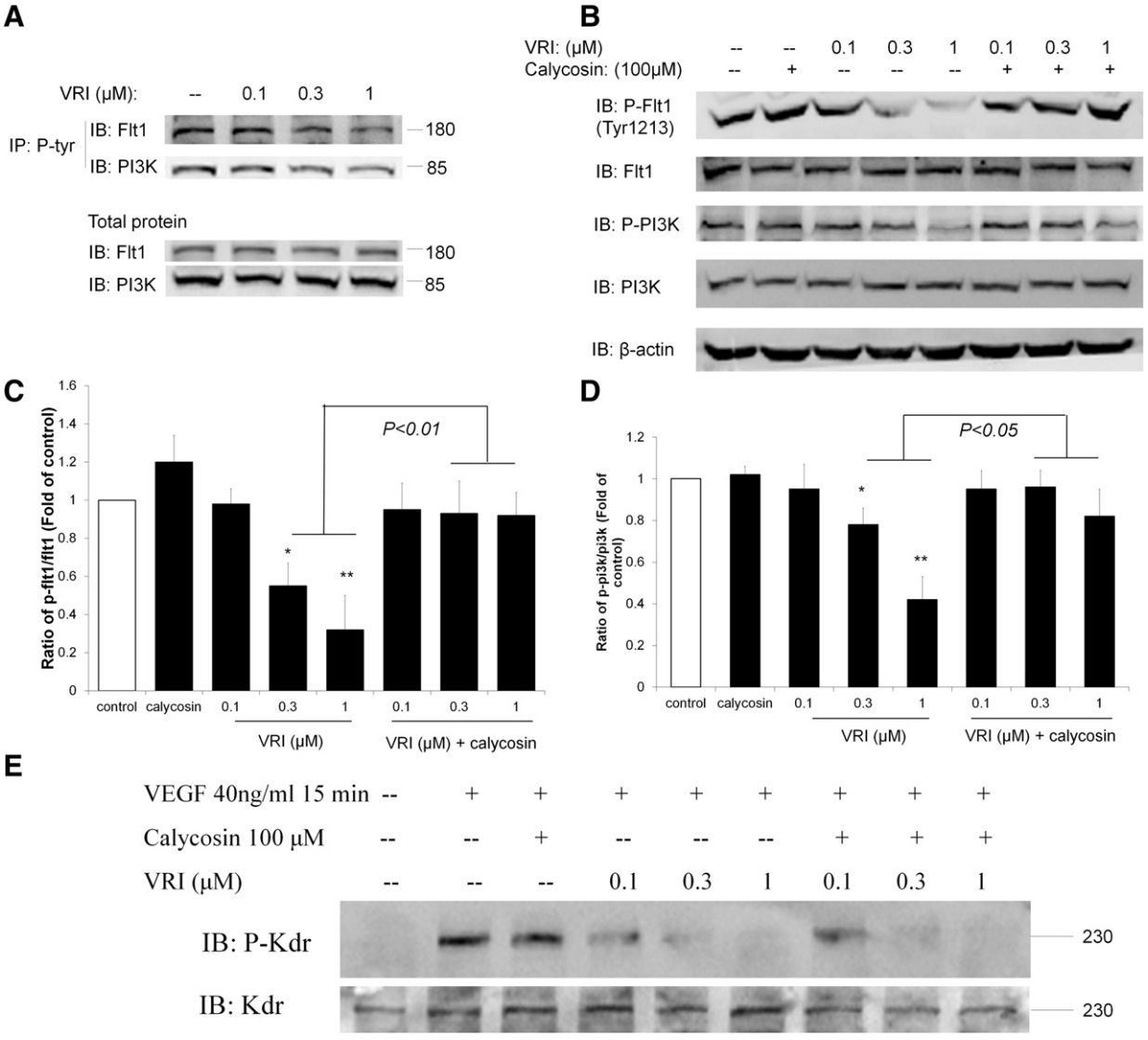

Fig. 4. Calycosin co-treatment abrogated VRI-induced inhibition on Flt1-dependent PI3K pathway. (A) Blot detecting Flt1 and PI3K in HUVECs treated with 0.1, 0.3 and 1 μM of VRI for 1 h and subjected to immunoprecipitation (IP) with an anti-Tyr antibody. Untreated cells served as controls. Total lysates were probed for total Flt1 and PI3K (loading control). (B–D) Quiescent HUVECs were treated with VRI (1 h) with or without the presence of calycosin. Western blot analysis showed that calycosin was able to restore for the phosphorylation of Flt1 tyrosine residue autophosphorylation site (Tyr1213) and its downstream effector PI3K. The bar graph represented quantitative analysis of 3 independent experiments, mean ± SD, $^{*}P < 0.05$ vs control. (D) Calycosin showed no effect on VRI-induced Kdr-TK inhibition.

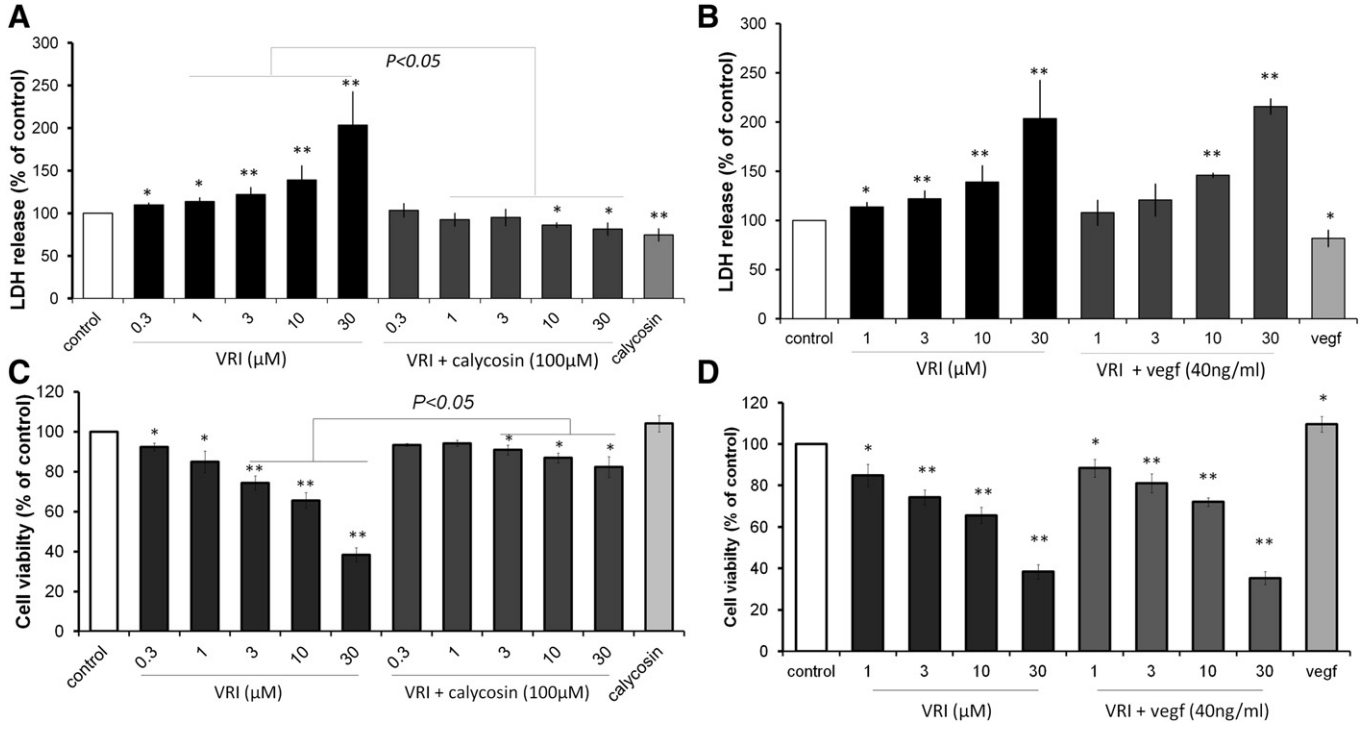

Fig. 5. Calycosin co-treatment abrogated VRI-induced HUVEC cytotoxicity. Quiescent HUVECs were treated with VRI (1 h) with or without the presence of calycosin (100 μM) or VEGF (40 ng/ml) for 24 h. (A–B) Comparison of VRI-induced LDH release in HUVEC in the presence of either calycosin or VEGF. (C–D) Comparison of VRI-induced cell cytotoxicity evaluated by XTT assay in HUVEC in the presence of either calycosin or VEGF. Quantitative analysis of 3 independent experiments, mean ± SD. $^{*}P < 0.05$; $^{**}P < 0.01$ vs control.

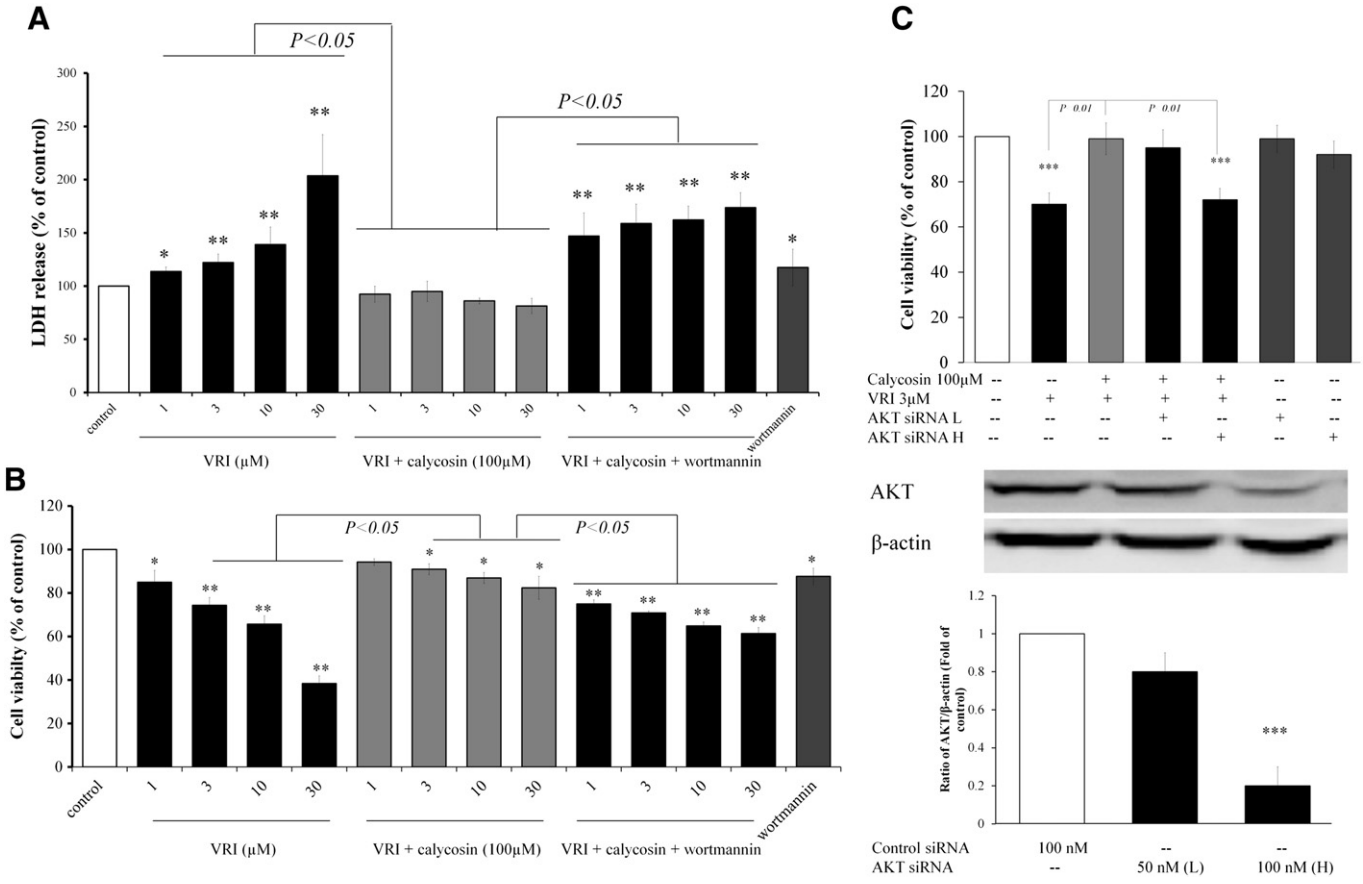

Fig. 6. Wortmannin (PI3K inhibitor) and AKT siRNA attenuated the abrogative effects of calycosin on VRI-induced cytotoxicity in HUVECs. HUVECs were treated with VRI (24 h) in the presence of calycosin (100 μM) and/or wortmannin (100 nM). HUVECs were transfected with AKT siRNA for 48 h and treated with VRI (24 h) in the presence of calycosin (100 μM). HUVEC viability and cytotoxicity were detected by (A) XTT assay and (B) LDH assay respectively. (C) AKT siRNA inhibited calycosin co-treatment abrogated VRI-induced HUVEC cytotoxicity. The efficiency of AKT siRNA transfection has been confirmed by Western blotting (D). Quantitative analysis of 3 independent experiments, mean ± SD, $^{*}P < 0.05$, $^{**}P < 0.01$ vs control.

against VRI for binding at Flt1 and thus modulated downstream cell survival signaling pathway including PI3K/AKT activity.

3.4. Flt1-dependent PI3K/AKT activity, but not Kdr-dependent, was involved in the abrogation of VRI-induced endothelial cell apoptosis and blood vessel loss by calycosin co-treatment in zebrafish embryos

TUNEL staining of normal *Tg(fli-1:EGFP)* zebrafish embryos at 32 hpf (Fig. 7A, a, Aa) showed that there was minimal evidence of endothelial cell apoptosis. VRI treatment (300 nM for 8 h in 24 hpf zebrafish embryos) induced significant endothelial cell apoptosis in intersegmental vessels (ISVs) and dorsal longitudinal anastomotic vessels (DLAVs) (Fig. 7B, b, Bb). This observation was consistent with previous study [11] that PTK787/ZK222584 (a VEGF receptor inhibitor similar to VRI) induced apoptosis of endothelial cell at dorsal aorta and posterior cardinal vein. Calycosin co-treatment (100 μM) was able to attenuate the VRI-induced endothelial cell apoptosis (Fig. 7C, c, Cc). Furthermore, this effect of calycosin was blocked by wortmannin (1 μM) (a PI3-kinase inhibitor) (Fig. 7D, d, Dd), while wortmannin alone did not induce any endothelial cell apoptosis (Fig. 7E, e, Ee).

Consistent with the results above, calycosin co-treatment was able to abolish VRI-induced blood vessel loss in zebrafish embryos in a dose-dependent manner (Fig. 8C to F). VRI (300 nM for 24 h) caused significant impairments of blood vessel development in intersegmental vessels (ISVs), dorsal longitudinal anastomotic vessels (DLAVs) and subintestinal vessels (SIVs) in 48 hpf zebrafish embryos (Fig. 8B). In addition, we observed that calycosin was much more effective in abolishing blood vessel impairments induced by non-selective (Flt1 and Kdr) inhibitors rather than selective Kdr inhibitors (Suppl. Fig. 2). Also, calycosin co-treatment was much more effective than calycosin post-treatment (after washout following VRI incubation) in abrogation of VRI-induced blood vessel loss (Suppl. Fig. 3).

3.5. Calycosin impeded VRI-induced blood vessel loss via Flt1 in zebrafish embryos

Flt1 expression was knocked down by injecting an ATG-targeting into morpholino (MO) Tg(*fli-1a*:EGFP)^{y1} zebrafish embryos (Fig. 9) and reduced Flt1 protein level (Fig. 9F). This resulted in excessive branching of segmental vessels (Fig. 9A`, D`, yellow arrows). Consistent with the results above, calycosin co-treatment was able to impede VRI-induced blood vessel loss in zebrafish embryos in standard control MO injected embryos (Fig. 9C). However, knockdown of Flt1 abolished the minimizing effects of calycosin on VRI-induced blood vessel loss in zebrafish embryos (Fig. 9C`).

3.6. VRI down-regulated the expressions of endothelial markers and calycosin co-treatment reversed it possibly via the restoration of basal Flt1-TK activity

Fig. 10 represented the gene expression levels of six key endothelial cells and angiogenesis markers in 48 hpf zebrafish embryos with real-time PCR analysis after the incubation (24 h) with VRI (30, 100, 300 μM) in the absence or presence of calycosin (100 μM). It was observed that VRI only dose-dependently down-regulated the gene expressions of *flt1*, *kdr*, *kdr1*, *vwf* and *cdh5* but up-regulated *vegfa*. Calycosin on its own induced a moderate increase of the endothelial markers. When calycosin was co-administered with VRI, it abrogated VRI-induced down-regulations of *flt1*, *kdr*, *kdr1*, *vwf* and *cdh5* significantly.

4. Discussion

In this study we attempted to dissect the role(s) of Flt1 (VEGFR-1) tyrosine kinase (TK) activity from that of Kdr (VEGFR-2/Flk1) in the regulation of blood vessel development in zebrafish embryos. We showed that under the circumstance when Kdr-TK activity was suppressed, basal level of Flt1-TK activity was unmasked and contributed significantly in endothelial cell (EC) survival and blood vessel formation. It is commonly believed that the major role(s) of Flt1 is to act as "VEGF-traps" by sFlt1 (secretory form of Flt1 that does not possess tyrosine kinase activity). However, results from this study provided novel evidences of Flt1-TK activation as a significant positive regulator in angiogenesis in zebrafish embryo angiogenesis.

Since Kdr is identified as the predominate regulator in angiogenesis, it was rather unexpected that Kdr-selective inhibitors caused significantly less severe blood vessel loss in zebrafish embryos than non-selective VEGF receptor inhibitors (which inhibit both Flt1 and Kdr). Based on this observation, we hypothesized that Flt1 possesses a more important role in blood vessel development in zebrafish than previously thought. The non-selective VEGF receptor inhibitor VRI caused the most severe blood vessel loss, treatment of 300 nM VRI for 24 h abolished all

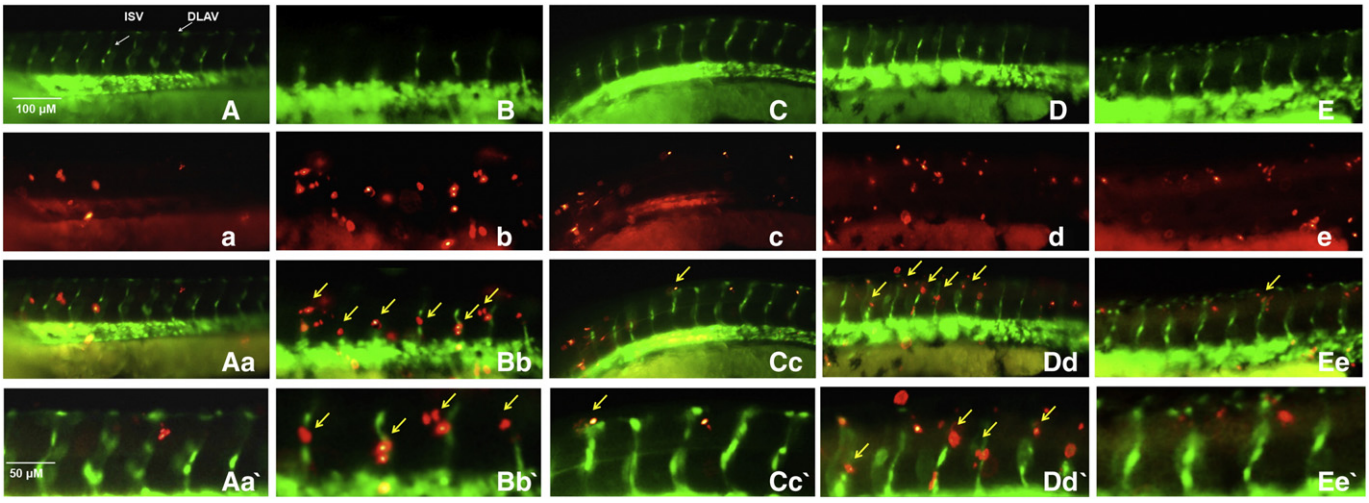

Fig. 7. TUNEL staining of *Tg(fli-1:EGFP)* zebrafish embryo endothelial cell apoptosis (red) in relation to blood vessels (green). (A, a, Aa, Aa`) Minimal endothelial cell (EC) apoptosis was observed in 32 hpf zebrafish embryos with no drug treatment. (B, b, Bb, Bb`) VRI treatment (300 nM for 8 h) in 24 hpf zebrafish embryos caused a significant increase of EC apoptosis in ISVs (intersegmental vessels) and DLAVs (dorsal longitudinal anastomotic vessels). (C, c, Cc, Cc`) Calycosin co-treatment (100 μM) attenuated VRI-induced endothelial apoptosis. (D, d, Dd, Dd`) Wortmannin (1 μM) abolished the effect of calycosin co-treatment. (E, e, Ee, Ee`) Wortmannin (1 μM) alone showed no significant effect on vascular development. Yellow arrows indicated apoptotic endothelial cells.

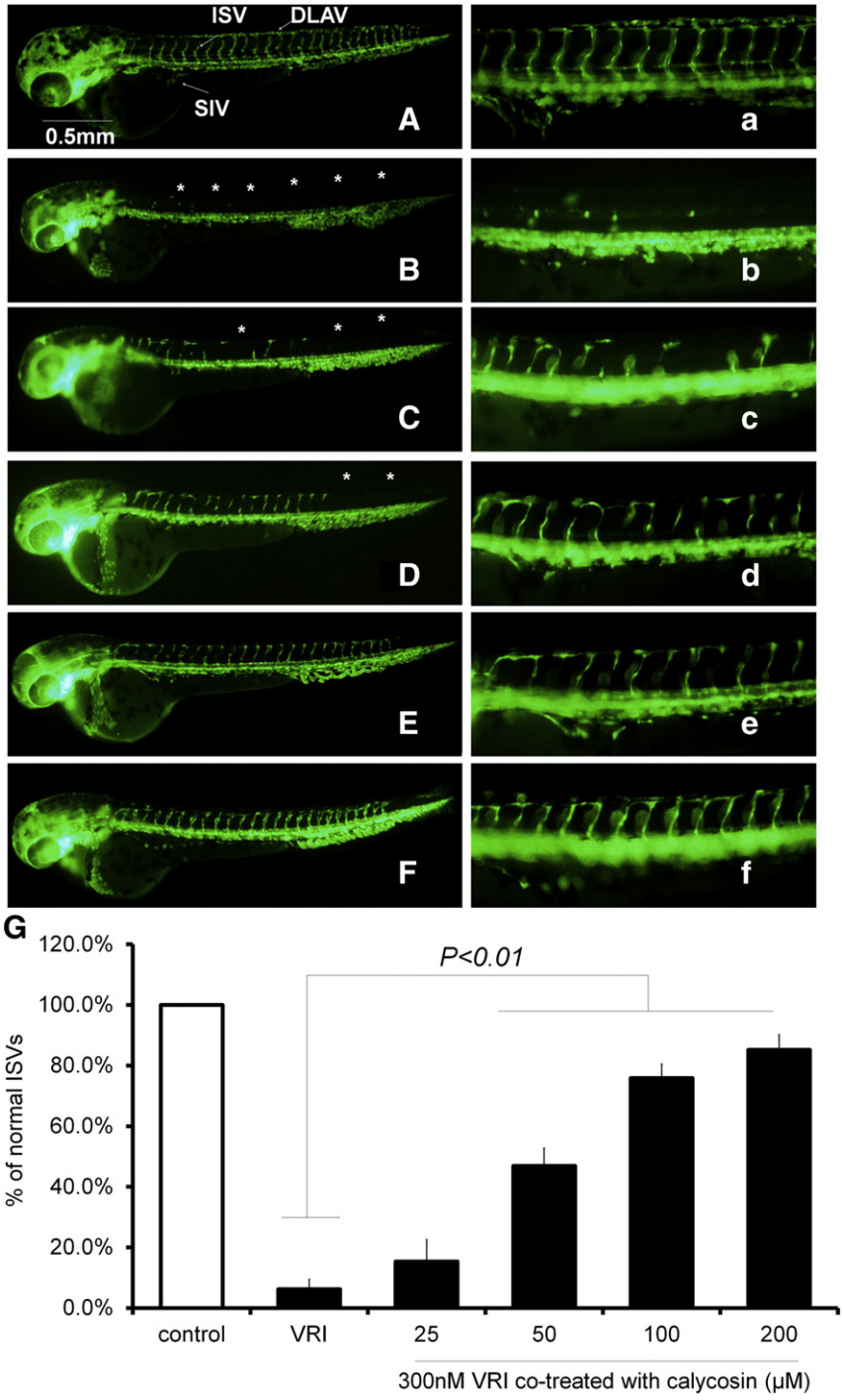

Fig. 8. Co-treatment of calycosin dose-dependently abolished VRI-induced blood vessel loss in zebrafish embryos. Effects of co-treatment of calycosin (25 to 200 μM) on VRI-induced blood vessel loss were evaluated in 48hpf Tg(*fli-1a*:EGFP)^{y1} zebrafish. Zebrafish embryos (24 hpf) were treated with (A-a) 0.1% DMSO (control), (B-b) VRI (300 nM), (C to F) various concentrations of calycosin (25, 50, 100, 200 μM) co-treated with VRI (300 nM) for 24 h. Live fluorescence microscopy highlighted EGFP expressing intersegmental blood vessels (ISVs), subintestinal vessels (SIVs) and dorsal longitudinal anastomotic vessels (DLAVs). White asterisks indicated blood vessel loss in ISV, SIV and DLAV regions. Scale bar = 500 μm. Quantitative analysis of 3 independent experiments, mean ± SD, $^{*}P < 0.05$, $^{**}P < 0.01$ vs control.

the blood vessel formation in zebrafish; thus it was chosen for further study. With molecular docking analysis and enzymatic assays we identified that calycosin behaved as a competitive ligand with high affinity for Flt1 and competed against VRI at a site without interfering its ATP-binding site and thus its kinase activation. On the contrary, molecular docking showed that calycosin could bind at Kdr activation segment but only very weakly. Nevertheless, in the present study, calycosin would not be able to interfere with Kdr-VRI binding since Kdr has a much higher affinity for VRI. Enzymatic assays and in vitro studies in HUVECs further confirmed the ability of calycosin to restore Flt1-TK autophosphorylation and activation by competing with VRI. This action of calycosin was specific for Flt1 and was not observed for Kdr. Data from others and our own have shown that the autophosphorylation of Flt1 was not affected by the binding of VEGF-A [15], and it has been debated that Flt1 autophosphorylation has other roles in vascular development. In particular, little was known about the role of Flt1 in the regulation of angiogenesis in early embryogenesis. It has been observed that although the deletion of tyrosine kinase (TK) domain in *flt1*$^{TK-/-}$

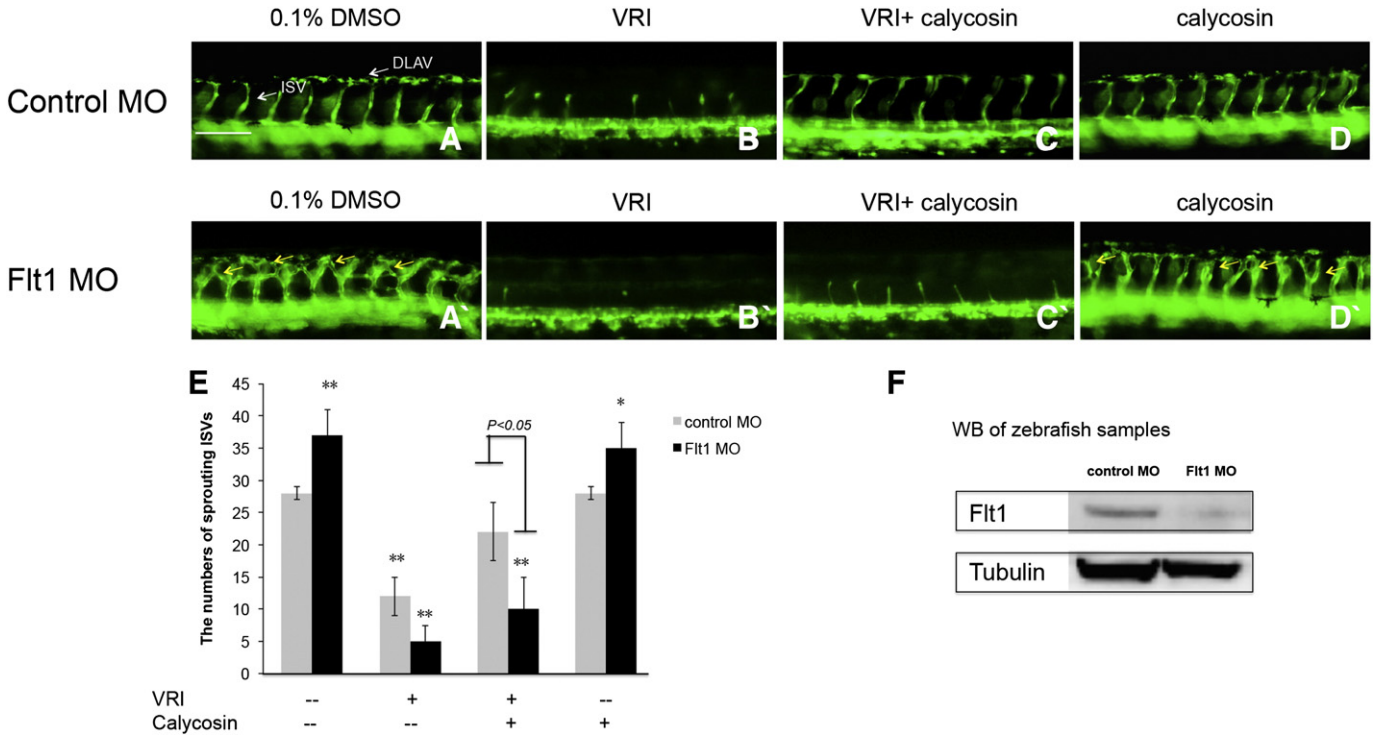

Fig. 9. The minimizing effect of calycosin on VRI-induced blood vessel loss was absent in zebrafish embryos injected with Flt1 MO. Tg(*fli-1a*:EGFP)^{y1} (24 hpf) zebrafish embryos were injected with (A–D) control MO and (A`–D`) Flt1 MO. (B, B`) VRI (300 nM, 24 h) induced blood vessel loss in the ISV and DLAV. (C, C`) Co-treatment of calycosin (100 μM) did not reverse the effect of VRI in Flt1 deficient background. (A, D) Calycosin treatment alone did not cause significant difference in vessel morphology in embryos injected with control MO. (A`, D`) Excessive segmental vessel branching was observed in zebrafish Flt1 morphants. (E) Statistical analysis showing that the effects of calycosin was absent in Flt1 morphants without any significant difference between the effects of VRI alone and VRI + calycosin. (F) Western blot showing the reduction of Flt1 protein level in Flt1 morphants. The yellow arrows in A` and D` indicate the aberrant connection between adjacent segmental vessels. Scale bar = 200 μm. Quantitative analysis of 3 independent experiments, mean ± SD, $^{*}P < 0.05$, $^{**}P < 0.01$ vs control MO.

mice did not affect normal development and angiogenesis, further deletion of the transmembrane (TM) domain in *flt1*$^{\text{TM-TK}-/-}$ resulted in 50% lethality due to impaired vascular development [32]. More recently, it has been shown that the down-regulation of Flt1 in HRMVECs (human retinal microvascular endothelial cells) modestly suppressed the VEGF-A-induced Src-PLD1-PKCγ-cPLA2 activation in Kdr and caused a reduction in DNA synthesis, migration and tube formation [33]. Indeed, our previous studies have shown that calycosin has modest proangiogenic effects by interaction with estrogen receptors [18,19]. In order to discard the possibility of calycosin acting via estrogen receptors, we used estrogen receptor antagonist (ICI 182,780) co-treated with calycosin and VRI. Results indicate that ICI 182,780 was unable to attenuate any calycosin effects in VRI-induced blood vessel loss (data not shown), indicating estrogen receptor independence.

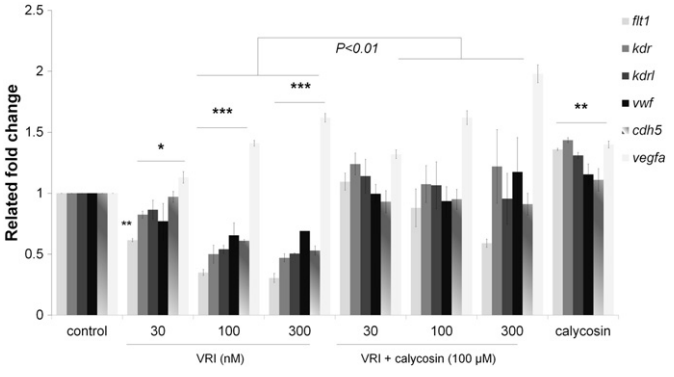

Fig. 10. VRI down-regulated the gene expressions of endothelial markers *flt1*, *kdr*, *kdr1*, *vwf* and *cdh5* in zebrafish embryos. 1 dpf zebrafish embryos treated with VRI (30, 100 and 300 nM) and/or calycosin (100 μM) for 24 h. VRI significantly down-regulated *flt1*, *kdr*, *kdr1*, *vwf* and *cdh5* expressions that were abrogated by calycosin co-treatment. Quantitative analysis of 3 independent experiments, mean ± SD, $^{*}P < 0.05$, $^{**}P < 0.01$ and $^{***}P < 0.001$ vs control.

Data from in vitro studies in HUVECs and in vivo studies in zebrafish embryos both demonstrated that restoration of basal Flt1-TK/PI3K activity prevented endothelial cell (EC) apoptosis induced by VRI and further reversed the loss of blood vessel formation caused by VRI action, even though Kdr activity was still completely suppressed by VRI. Some studies suggested that Flt1 appears to be involved in the regulation VEGF-induced endothelial cell migration, invasion and cell growth via recruitment of the PI3K/Akt signaling pathway [14,13]. However, here in the present study we observed that the autophosphorylation and activation of Flt1 as well as the effects of calycosin in rescuing EC apoptosis and blood vessel loss were all VEGF-A-independent.

Quantitative analysis of using image analysis and q-PCR further demonstrated the minimizing effects of calycosin on VRI-induced vascular defects in a dose-dependent manner. Interestingly, this effect of calycosin was blocked by wortmannin, suggesting the involvement of PI3K pathway. Furthermore, knockdown of Flt1 by morpholino in zebrafish showed that in a Flt1 deficient background, the minimizing effect of calycosin on VRI-induced vascular defects is absent. It is now well accepted that von Willebrand factor (vWF) and vascular endothelial cadherin (cdh5) are endothelail cell-specific markers. [34]. Thus, in the present study, the gene expressions of flt1, kdr, kdrl, vWF and cdh5 were evaluated as a quantitative measurement for blood vessel changes. The results showed that calycosin reversed VRI decreased flt1, kdr, kdrl, vWF and cdh5 gene expression indicating that calycosin

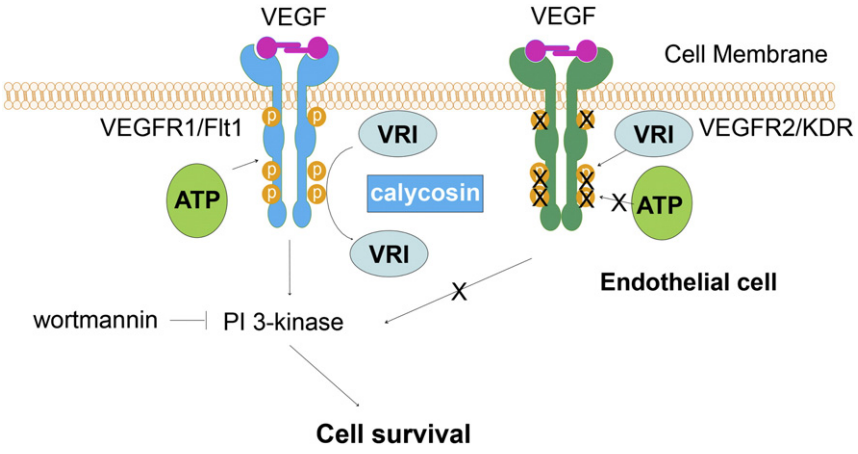

Fig. 11. Schematic diagram of Flt1 and Kdr tyrosine kinase activities and their relation with VRI and calycosin.

rescued VRI-induced endothelial cell loss in zebrafish embryos. Vegfa is a fundamental mediator of physiological and pathophysiological angiogenesis [35]. Interestingly, our results showed that Vegfa is upregulated in VRI treatment in a concentration dependent manner. Moreover, calycosin enhanced Vegfa upregulated in VRI treatment. It has been shown that VEGF is produced not only by endothelial cells but also by smooth muscle cells [36]. In our previous studies we found that some anti-angiogenic compounds hat are anti-angiogeneic in zebrafish also dose-dependently induced Vegfa mRNA expression [37,38]. It is possible that the increase in Vegfa expression could be because of a feedback regulation resulting from the blood vessel loss induced by VRI.

In conclusion, VRI strongly inhibited physiological functions of VEGF receptors and suppressed endothelial cell survival in vitro and in vivo. This resulted in blood vessel loss in zebrafish embryos and induced endothelial cell cytotoxicity in HUVECs. Interestingly, calycosin cotreatment abrogated VRI-induced blood vessel loss in zebrafish embryos and cytotoxicity in HUVECs. Docking and kinase inhibition assay revealed that calycosin competed with VRI for the TK domain of Flt1 without affecting ATP binding. Meanwhile, calycosin did not affect the interaction between VRI and Kdr-TK. Consistent with these results, calycosin counteracted the inhibition of Flt1-TK and PI3K phosphorylation induced by VRI in HUVECs. Further studies in vitro and in vivo showed that wortmannin, a PI3K inhibitor and AKT siRNA blocked the abrogation of VRI-mediated endothelial cytotoxicity by calycosin. The quantitative analysis of calycosin rescues effects by using image analysis and q-PCR with endothelial cell-specific marker gene expression ((Fig. 11). Taken together, we postulate that there might be a basal level of Flt1-TK/PI3K/Akt activity for maintaining physiological angiogenesis in zebrafish embryos.

Author contribution

SL, MPMH, SMYL, YWK, SWC and GPHL conceived and designed the experiments. SL, XLZ and YYD performed the experiments. SL, XLZ and YYD analyzed the data and wrote the manuscript.

Acknowledgements

This work was supported by grants from the Science and Technology Development Fund Macao SAR, China (Ref. No. 014/2011/A1), Overseas and Hong Kong, Macau Young Scholars Collaborative Research Fund by the Natural National Science Foundation of China (Grant No. 81328025) and Research Committee of University of Macau.

Appendix A. Supplementary data

Supplementary data to this article can be found online at http://dx.doi.org/10.1016/j.bbagen.2014.10.023.

References

[1] H. Habeck, J. Odenthal, B. Walderich, H. Maischein, S. Schulte-Merker, Analysis of a zebrafish VEGF receptor mutant reveals specific disruption of angiogenesis, Curr. Biol. 12 (2002) 1405–1412.
[2] G.H. Fong, J. Rossant, M. Gertsenstein, M.L. Breitman, Role of the Flt-1 receptor tyrosine kinase in regulating the assembly of vascular endothelium, Nature 376 (1995) 66–70.
[3] S. Koch, S. Tugues, X. Li, L. Gualandi, L. Claesson-Welsh, Signal transduction by vascular endothelial growth factor receptors, Biochem. J. 437 (2011) 169–183.
[4] F. Shalaby, J. Rossant, T.P. Yamaguchi, M. Gertsenstein, X.F. Wu, M.L. Breitman, A.C. Schuh, Failure of blood-island formation and vasculogenesis in Flk-1-deficient mice, Nature 376 (1995) 62–66.
[5] P. Carmeliet, N. Mackman, L. Moons, T. Luther, P. Gressens, I. Van Vlaenderen, H. Demunck, M. Kasper, G. Breier, P. Evrard, M. Muller, W. Risau, T. Edgington, D. Collen, Role of tissue factor in embryonic blood vessel development, Nature 383 (1996) 73–75.
[6] A. Shinkai, M. Ito, H. Anazawa, S. Yamaguchi, K. Shitara, M. Shibuya, Mapping of the sites involved in ligand association and dissociation at the extracellular domain of the kinase insert domain-containing receptor for vascular endothelial growth factor, J. Biol. Chem. 273 (1998) 31283–31288.
[7] M. Shibuya, Structure and dual function of vascular endothelial growth factor receptor-1 (Flt-1), Int. J. Biochem. Cell Biol. 33 (2001) 409–420.
[8] S. Hiratsuka, O. Minowa, J. Kuno, T. Noda, M. Shibuya, Flt-1 lacking the tyrosine kinase domain is sufficient for normal development and angiogenesis in mice, Proc. Natl. Acad. Sci. U. S. A. 95 (1998) 9349–9354.
[9] N.C. Kappas, G. Zeng, J.C. Chappell, J.B. Kearney, S. Hazarika, K.G. Kallianos, C. Patterson, B.H. Annex, V.L. Bautch, The VEGF receptor Flt-1 spatially modulates Flk-1 signaling and blood vessel branching, J. Cell Biol. 181 (2008) 847–858.
[10] N. Bahary, K. Goishi, C. Stuckenholz, G. Weber, J. Leblanc, C.A. Schafer, S.S. Berman, M. Klagsbrun, L.I. Zon, Duplicate VegfA genes and orthologues of the KDR receptor tyrosine kinase family mediate vascular development in the zebrafish, Blood 110 (2007) 3627–3636.
[11] J. Chan, P.E. Bayliss, J.M. Wood, T.M. Roberts, Dissection of angiogenic signaling in zebrafish using a chemical genetic approach, Cancer Cell 1 (2002) 257–267.
[12] J. Cai, S. Ahmad, W.G. Jiang, J. Huang, C.D. Kontos, M. Boulton, A. Ahmed, Activation of vascular endothelial growth factor receptor-1 sustains angiogenesis and Bcl-2 expression via the phosphatidylinositol 3-kinase pathway in endothelial cells, Diabetes 52 (2003) 2959–2968.
[13] F. Wang, M. Yamauchi, M. Muramatsu, T. Osawa, R. Tsuchida, M. Shibuya, RACK1 regulates VEGF/Flt1-mediated cell migration via activation of a PI3K/Akt pathway, J. Biol. Chem. 286 (2011) 9097–9106.
[14] W.D. Zhao, W. Liu, W.G. Fang, K.S. Kim, Y.H. Chen, Vascular endothelial growth factor receptor 1 contributes to *Escherichia coli* K1 invasion of human brain microvascular endothelial cells through the phosphatidylinositol 3-kinase/Akt signaling pathway, Infect. Immun. 78 (2010) 4809–4816.
[15] N. Ito, C. Wernstedt, U. Engstrom, L. Claesson-Welsh, Identification of vascular endothelial growth factor receptor-1 tyrosine phosphorylation sites and binding of SH2 domain-containing molecules, J. Biol. Chem. 273 (1998) 23410–23418.
[16] Y. Yu, J.D. Hulmes, M.T. Herley, R.G. Whitney, J.W. Crabb, J.D. Sato, Direct identification of a major autophosphorylation site on vascular endothelial growth factor

receptor Flt-1 that mediates phosphatidylinositol 3′-kinase binding, Biochem. J. 358 (2001) 465–472.
[17] S.A. Cunningham, M.N. Waxham, P.M. Arrate, T.A. Brock, Interaction of the Flt-1 tyrosine kinase receptor with the p85 subunit of phosphatidylinositol 3-kinase. Mapping of a novel site involved in binding, J. Biol. Chem. 270 (1995) 20254–20257.
[18] S. Li, S. Lou, B.U. Lei, T.F. Chan, Y.W. Kwan, S.W. Chan, G.P. Leung, S.K. Tsui, S.M. Lee, Transcriptional profiling of angiogenesis activities of calycosin in zebrafish, Mol. Biosyst. 7 (2011) 3112–3121.
[19] J.Y. Tang, S. Li, Z.H. Li, Z.J. Zhang, G. Hu, L.C. Cheang, D. Alex, M.P. Hoi, Y.W. Kwan, S.W. Chan, G.P. Leung, S.M. Lee, Calycosin promotes angiogenesis involving estrogen receptor and mitogen-activated protein kinase (MAPK) signaling pathway in zebrafish and HUVEC, PLoS One 5 (2010) e11822.
[20] M. Westerfield, The zebrafish book, A Guide for the Laboratory Use of Zebrafish (*Danio rerio*)3rd Edition, University of Oregon Press, Eugene, OR, 1995. 385.
[21] O. Trott, A.J. Olson, AutoDock Vina: improving the speed and accuracy of docking with a new scoring function, efficient optimization, and multithreading, J. Comput. Chem. 31 (2010) 455–461.
[22] X. Zhou, Y. Wang, T. Hu, P.M. Or, J. Wong, Y.W. Kwan, D.C. Wan, P.M. Hoi, P.B. Lai, J.H. Yeung, Enzyme kinetic and molecular docking studies for the inhibitions of miltirone on major human cytochrome P450 isozymes, Phytomedicine 20 (2013) 367–374.
[23] J. Krueger, D. Liu, K. Scholz, A. Zimmer, Y. Shi, C. Klein, A. Siekmann, S. Schulte-Merker, M. Cudmore, A. Ahmed, F. le Noble, Flt1 acts as a negative regulator of tip cell formation and branching morphogenesis in the zebrafish embryo, Development 138 (2011) 2111–2120.
[24] J.M. Wood, G. Bold, E. Buchdunger, R. Cozens, S. Ferrari, J. Frei, F. Hofmann, J. Mestan, H. Mett, T. O'Reilly, E. Persohn, J. Rosel, C. Schnell, D. Stover, A. Theuer, H. Towbin, F. Wenger, K. Woods-Cook, A. Menrad, G. Siemeister, M. Schirner, K.H. Thierauch, M.R. Schneider, J. Drevs, G. Martiny-Baron, F. Totzke, D. Marme, PTK787/ZK 222584, a novel and potent inhibitor of vascular endothelial growth factor receptor tyrosine kinases, impairs vascular endothelial growth factor-induced responses and tumor growth after oral administration, Cancer Res. 60 (2000) 2178–2189.
[25] L. Sun, N. Tran, F. Tang, H. App, P. Hirth, G. McMahon, C. Tang, Synthesis and biological evaluations of 3-substituted indolin-2-ones: a novel class of tyrosine kinase inhibitors that exhibit selectivity toward particular receptor tyrosine kinases, J. Med. Chem. 41 (1998) 2588–2603.
[26] L. Sun, N. Tran, C.X. Liang, F. Tang, A. Rice, R. Schreck, K. Waltz, L.K. Shawver, G. McMahon, C. Tang, Design, synthesis, and evaluations of substituted 3-[(3-or 4-carboxyethylpyrrol-2-yl)methylidenyl]indolin-2-ones as inhibitors of VEGF, FGF, and PDGF receptor tyrosine kinases, J. Med. Chem. 42 (1999) 5120–5130.
[27] G. Aparicio-Gallego, M. Blanco, A. Figueroa, R. Garcia-Campelo, M. Valladares-Ayerbes, E. Grande-Pulido, L. Anton-Aparicio, New insights into molecular mechanisms of Sunitinib-associated side effects, Mol. Cancer Ther. 10 (2011) 2215–2223.
[28] L. Sun, C. Liang, S. Shirazian, Y. Zhou, T. Miller, J. Cui, J.Y. Fukuda, J.Y. Chu, A. Nematalla, X.Y. Wang, H. Chen, A. Sistla, T.C. Luu, F. Tang, J. Wei, C. Tang, Discovery of 5-[5-fluoro-2-oxo-1,2-dihydroindol-(3Z)-ylidenemethyl]-2,4-dimethyl-1H-pyrrole-3-carboxylic acid (2-diethylaminoethyl)amide, a novel tyrosine kinase inhibitor targeting vascular endothelial and platelet-derived growth factor receptor tyrosine kinase, J. Med. Chem. 46 (2003) 1116–1119.
[29] L. Sun, N. Tran, C.X. Liang, S. Hubbard, F. Tang, K. Lipson, R. Schreck, Y. Zhou, G. McMahon, C. Tang, Identification of substituted 3-[(4,5,6,7-tetrahydro-1H-indol-2-yl)methylene]-1,3-dihydroindol-2-ones as growth factor receptor inhibitors for VEGF-R2 (Flk-1/KDR), FGF-R1, and PDGF-R beta tyrosine kinases, J. Med. Chem. 43 (2000) 2655–2663.
[30] A.P. Kornev, N.M. Haste, S.S. Taylor, L.F. Eyck, Surface comparison of active and inactive protein kinases identifies a conserved activation mechanism, Proc. Natl. Acad. Sci. U. S. A. 103 (2006) 17783–17788.
[31] R. Roskoski Jr., VEGF receptor protein-tyrosine kinases: structure and regulation, Biochem. Biophys. Res. Commun. 375 (2008) 287–291.
[32] S. Hiratsuka, K. Nakao, K. Nakamura, M. Katsuki, Y. Maru, M. Shibuya, Membrane fixation of vascular endothelial growth factor receptor 1 ligand-binding domain is important for vasculogenesis and angiogenesis in mice, Mol. Cell. Biol. 25 (2005) 346–354.
[33] N.K. Singh, D.E. Hansen, V. Kundumani-Sridharan, G.N. Rao, Both Kdr and Flt1 play a vital role in hypoxia-induced Src-PLD1-PKC gamma-cPLA(2) activation and retinal neovascularization, Blood 121 (2013) 1911–1923.
[34] L. Zanetta, S.G. Marcus, J. Vasile, M. Dobryansky, H. Cohen, K. Eng, P. Shamamian, P. Mignatti, Expression of von Willebrand factor, an endothelial cell marker, is up-regulated by angiogenesis factors: a potential method for objective assessment of tumor angiogenesis, Int. J. Cancer (J. Int. Cancer), 85 (2000) 281–288.
[35] E. Tischer, R. Mitchell, T. Hartman, M. Silva, D. Gospodarowicz, J.C. Fiddes, J.A. Abraham, The human gene for vascular endothelial growth factor. Multiple protein forms are encoded through alternative exon splicing, J. Biol. Chem. 266 (1991) 11947–11954.
[36] M. Inoue, H. Itoh, M. Ueda, T. Naruko, A. Kojima, R. Komatsu, K. Doi, Y. Ogawa, N. Tamura, K. Takaya, T. Igaki, J. Yamashita, T.H. Chun, K. Masatsugu, A.E. Becker, K. Nakao, Vascular endothelial growth factor (VEGF) expression in human coronary atherosclerotic lesions: possible pathophysiological significance of VEGF in progression of atherosclerosis, Circulation 98 (1998) 2108–2116.
[37] I.K. Lam, D. Alex, Y.H. Wang, P. Liu, A.L. Liu, G.H. Du, S.M. Lee, In vitro and in vivo structure and activity relationship analysis of polymethoxylated flavonoids: identifying sinensetin as a novel antiangiogenesis agent, Mol. Nutr. Food Res. 56 (2012) 945–956.
[38] K.H. Lam, D. Alex, I.K. Lam, S.K. Tsui, Z.F. Yang, S.M. Lee, Nobiletin, a polymethoxylated flavonoid from citrus, shows anti-angiogenic activity in a zebrafish in vivo model and HUVEC in vitro model, J. Cell. Biochem. 112 (2011) 3313–3321.